Multienzyme Chemiluminescent Foldable Biosensor for On-Site Detection of Acetylcholinesterase Inhibitors

Laura Montali , Maria Maddalena Calabretta , Antonia Lopreside , Marcello D'Elia , Massimo Guardigli , Elisa Michelini

Epub 2020 Apr 29

Cite this article as: Montali L, Calabretta MM, Lopreside A, D'Elia M, Guardigli M, Michelini E. Multienzyme chemiluminescent foldable biosensor for on-site detection of acetylcholinesterase inhibitors. Biosens Bioelectron. 2020;162:112232. doi:10.1016/j.bios.2020.112232

Multienzyme chemiluminescent foldable biosensor for on-site detection of acetylcholinesterase inhibitors

Laura Montali[1◆], Maria Maddalena Calabretta[1◆], Antonia Lopreside[1], Marcello D'Elia[2], Massimo Guardigli*[1], Elisa Michelini*[1,3,4]

[1]Department of Chemistry "Giacomo Ciamician", University of Bologna, Via Selmi 2, 40126 Bologna, Italy

[2]Gabinetto Regionale di Polizia Scientifica per l'Emilia-Romagna, Via Volto Santo 3, 40123, Bologna, Italy

[3]INBB, Istituto Nazionale di Biostrutture e Biosistemi, 00136 Rome, Italy

[4]Health Sciences and Technologies-Interdepartmental Center for Industrial Research (HST-ICIR), University of Bologna, via Tolara di Sopra 41/E 40064, Ozzano dell'Emilia, Bologna, Italy

◆ These authors contributed equally.

*Corresponding authors:
Prof. Elisa Michelini
Dept. of Chemistry "Giacomo Ciamician"
Alma Mater Studiorum - University of Bologna
Via Selmi 2
40126-Bologna, Italy
Tel/Fax +39 051 343398
Cell: +39 338 6860955
E-mail: elisa.michelini8@unibo.it

Prof. Massimo Guardigli
Dept. of Chemistry "Giacomo Ciamician"
Alma Mater Studiorum - University of Bologna
Via Selmi 2
40126-Bologna, Italy
Tel/Fax +39 051 343398
E-mail: massimo.guardigli@unibo.it

Abstract

The rapid hydrolysis of acetylcholine (ACh), one of the key neurotransmitters in the human body, by the enzyme acetylcholinesterase (AChE) is fundamental for the termination of ACh impulse transmission. Several chemicals, including organophosphorus (OP) pesticides, warfare agents and drugs, are AChE reversible or irreversible inhibitors, thus their rapid on-site detection is of primary importance. Here we report for the first time a chemiluminescence (CL) foldable paper-based biosensor for detection of AChE inhibitors. The biosensor exploits three coupled enzymatic reactions catalysed by AChE, choline oxidase and horseradish peroxidase, leading to production of hydrogen peroxide, which is measured with an optimized luminol substrate. The origami approach allows to add reagents and trigger the sequential reactions in separate steps. A compact 3D-printed device including a mini dark box was created to enable smartphone detection. The CL foldable paper-based biosensor showed suitable for the rapid detection of OP pesticides in food matrices with a total assay time of 25 min. It is thus a rapid, low cost portable test suitable for point-of-need detection of chemicals inhibiting AChE.

Keywords: Chemiluminescence, Paper-based biosensor, Foldable biosensor, Smartphone, Acetylcholinesterase

1. INTRODUCTION

Acetylcholine (ACh) is one of the key neurotransmitters in the human body, acting as a chemical messenger for conveying signals through the nerve synapse. The impairment of central cholinergic transmission has been related to a plethora of diseases, including Alzheimer's disease, Parkinson's disease, schizophrenia, and epilepsy (Ahmed et al., 2019). In both the central and peripheral nervous systems, the termination of impulse transmission occurs via rapid ACh hydrolysis by the enzyme acetylcholinesterase (AChE). AChE converts ACh into choline and acetic acid, thus causing the return of a cholinergic neuron to its resting state. The enzyme can be inactivated by several inhibitors, leading to acetylcholine accumulation and disrupted neurotransmission caused by hyperstimulation of nicotinic and muscarinic receptors (Colović et al., 2013). Reversible AChE inhibitors are widely used for treating neurodegenerative diseases, while irreversible inhibitors are associated with toxic effects (Andreani et al., 2008). Irreversible AChE inhibitors include chemical warfare agents and many organophosphorus (OP) compounds used as pesticides and insecticides. These inhibitors deactivate AChE by a nucleophilic attack to the serine residue (Ser200) located in the active site, thus generating a phosphorylated enzyme. This inhibition causes accumulation of ACh with severe respiratory impairment, paralysis, and death (Patel and Sangeeta, 2019).

The rapid detection of these chemicals in water, soil, and food represents a major challenge to current analytical technologies. Apart from warfare agents, OP pesticides are among the most important environmental pollutants because of their increasing use in agriculture as insecticides, fungicides, herbicides, contributing for about 38% of the total employed pesticides (Pundir and Malik, 2019).

Most countries, including Europe, have fixed maximum residue levels (MRL) for food and animal feed. European legislation (Regulation EC 396/2005 and amendments) covers around 1100 pesticides currently or formerly used in agriculture in or outside the EU, with a general default MRL of 0.01 mg/kg. Recently, on 10 January 2020, the European Commission formally adopted two regulations to not renew the approvals of chlorpyrifos and chlorpyrifos-methyl. As a consequence, all Member

States should, within one month, withdraw all authorizations for plant protection products containing these active substances (https://ec.europa.eu/food/plant/pesticides/approval_active_substances/chlorpyrifos_chlorpyrifos-methyl_en). Since chlorpyrifos-methyl shows significant hepatotoxicity and nephrotoxicity, (Deng et al., 2016) its detection is of primary concern for agriculture workers and for the general population. Thanks to their excellent sensitivity, High Performance Liquid Chromatography (HPLC) and Gas Chromatography (GC) coupled to mass spectrometry (MS) are widely used for OP compounds detection (Samsidar et al., 2018; Garlito et al., 2019). However, these techniques require specialized laboratory and skilled personnel, thus are not suitable for on-site detection. After the pioneering work by G. Guilbault, (Guilbault et al., 1962) several successful examples of the use of AChE inhibition were reported to detect OP pesticides (Roda et al., 1994; Guardigli et al., 2005). Biosensors targeting AChE inhibition are being considered suitable approaches for real-time, cost-effective and on-field OP compounds monitoring (Pundir and Malik, 2019). Most biosensors for OP pesticide detection rely on fluorescence, electrochemiluminescence and electrochemical detection (Chang et al., 2016; Yao et al., 2019; Arduini et al., 2010; Arduini et al., 2019; Uniyal and Sharma, 2018; Huang et al., 2019), generally being amperometric biosensors those showing the lowest detection limits.

The possibility of implementing enzymatic assays with smartphone-based bio-chemiluminescence (BL-CL) detection has been explored by us and others (Roda et al., 2016; Roda et al., 2017; Huang et al., 2018; Calabretta et al., 2020). In recent years, smartphone-based biosensors have had an exponential growth as the integrated smartphone detector provides sufficient sensitivity to replace portable light detectors such as Charge-Coupled Devices (CCDs) and Complementary Metal Oxide Semiconductor (CMOS) sensors (Roda et al., 2014a; Cevenini et al., 2016).

Paper-based sensors were proposed for fabricating simple, low-cost, portable and disposable analytical devices suitable for clinical diagnosis, food and environmental monitoring (Meredith et al., 2016; Cinti, 2019; Zangheri et al., 2015; Liu et al. 2019). Thanks to its hydrophilic cellulose fiber

composition, paper is porous, enables passive liquid transport without the need of pumps and it is highly compatible with several types of reactions (Hu et al., 2014; López-Marzo and Merkoçi, 2016). Moreover, paper based analytical devices mimicking the origami art of paper folding are suitable alternatives for triggering the reactions catalyzed by specific enzymes during the folding (Liu et al. 2013). In 2012, Ge et al. developed a sandwich-type chemiluminescence immunoassay based on 3D origami device for the detection of tumor markers. This 3D origami-based immunodevice has the capability to separate the operational procedures into several steps including (i) folding pads above/below and (ii) addition of reagent/buffer under a specific sequence, showing excellent analytical performance for the simultaneous detection of four tumor markers (Ge et al., 2012). Very recently an origami-like paper-based electrochemical biosensor was developed to detect mustard agent simulants, achieving limits of detection of 1 mM and 0.019 $g \cdot min/m^3$ for the targets in liquid and aerosol phase, respectively (Colozza et al., 2019).

Till now, the implementation of CL as detection technique in origami-paper based biosensors has been seldomly explored, with only few examples mostly relying on immunoassays (Ge et al., 2012; Liu et al., 2013). While several CL biosensors based on enzymatic reactions have been developed (Li et al., 2019; Chen et al., 2016; Yeh et al., 2019), till now there are no examples of implementation of coupled enzyme reactions with CL detection into foldable paper-based smartphone biosensors. This approach benefits from the high detectability of CL signals and simplicity of use deriving from easy folding of the paper, providing an instrument-free biosensor that only requires a smartphone for detection.

In this work we propose a foldable paper-based biosensor with CL detection based on the origami technique. This biosensor is based on the inhibition process of AChE by molecules such as OP pesticides, nerve gases and some drugs. As regards the CL reaction, AChE activity is measured through a series of coupled enzymatic reactions exploiting AChE, choline oxidase (ChOx) and Horseradish Peroxidase (HRP) leading to light emission. When AChE is inhibited, there is a

decreased production of hydrogen peroxide, and consequently a reduction in light emission. An improved luminol substrate is also reported that provides improved sensitivity, possibly having broad applicability in CL-based biosensing.

2. EXPERIMENTAL SECTION

2.1 Materials and chemicals

Acetylcholinesterase (AChE) from *Electrophorus electricus* (EC 3.1.1.7), choline oxidase (ChOx) from *Alcaligenes sp.* (EC 1.1.3.17), peroxidase (HRP) Type VI-A from horseradish (EC 1.11.1.7), acetylcholine (ACh) chloride and luminol sodium salt were provided by Sigma Aldrich, St. Louis, MO, USA. Stock solutions of the enzymes (AChE: 100 U/mL in 20 mM Tris-HCl buffer pH 7.5; ChOx: 20 U/mL in 10 mM Tris-HCl buffer pH 8.0 containing 2.0 mM EDTA and 134 mM KCl; HRP: 108 U/mL in 20 mM Tris-HCl buffer pH 7.5) were prepared and stored at -20°C. Whatman 1 CHR cellulose chromatography paper from GE Healthcare (Chicago, IL, USA) was used for the origami paper-based analytical device. Commercial Reldan®22 insecticide containing 225 g/L of chlorpyrifos methyl was purchased from Corteva Agriscience (Wilmington, DE, USA). SuperSignal ELISA Femto Maximum Sensitivity was provided by Thermo Scientific (Waltham, Massachusetts, USA).

2.2 Design and fabrication of the foldable paper biosensor

The foldable biosensor pattern (Fig. 1a) was designed using PowerPoint (Microsoft, Redmond, WA, USA) and printed onto the Whatman 1 CHR chromatography paper using a ColorQube 8570 office wax printer (Xerox, Norwalk, CT, USA). The biosensor consisted of four circular hydrophilic "wells" (diameter 5 mm), numbered from 1 to 4 according to the folding sequence, surrounded by hydrophobic areas. After printing, the waxed pattern was cured for 1 min at 100 °C to allow wax to diffuse in the paper thickness to create the hydrophobic areas. Enzymes were then loaded in the biosensor by dispensing appropriate volumes of enzyme solutions in the wells (5 µL of a 100 U/mL

AChE solution in well No.1, 15 µL of a 20 U/mL ChOx solution in well No. 2, and 15 µL of a 108 U/mL HRP solution in well No. 3). Finally, the biosensor was let drying for 30 min at 37°C.

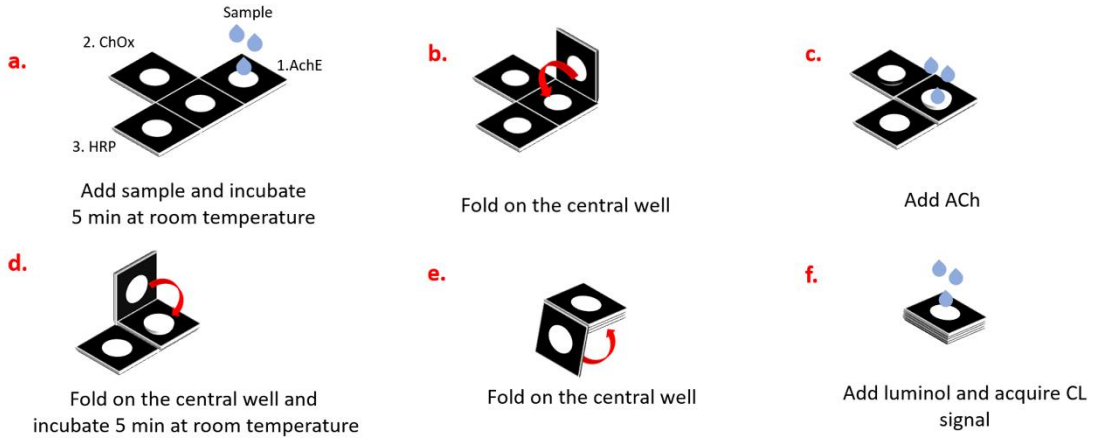

Fig. 1: Schematic representation of the foldable paper-based biosensor and assay procedure.

2.3 3D-printed analytical device

Accessories for performing the assay (i.e., a holder for the foldable paper biosensor and a mini dark box for CL imaging of the biosensor with a smartphone) were fabricated using a Replicator 2X 3D printer (Makerbot, Boston, MA, USA), which allows rapid prototyping of the device components by exploiting the Fused Deposition Modeling (FDM) technology. Three-dimensional models of device components were created using the SketchUp Free browser-based 3D design platform (Trimble, Sunnyvale, CA, USA) and saved in the stereolithography file format (STL). Then the proprietary software MakerWare v.2.4 (Makerbot) was used for slicing the 3D models (i.e., converting the 3D models into a series of thin layers for printing) and producing a file (X3G) with the appropriate printing instructions for the 3D printer. All components were printed in black acrylonitrile-butadiene-styrene copolymer ("True Black" ABS, Makerbot) at 250-µm layer thickness, 10% infill.

The holder for the paper biosensor (Fig. 2c) consisted of two parts (Fig.2d), which are held together by four N52 grade neodymium magnets (diameter 6 mm, thickness 2 mm), and was designed to keep the paper biosensor folded during the steps of the analytical procedure (Fig. 2e-f). Holes in the two parts of the holder allowed addition of luminol solution and imaging of the CL signal from the folded

biosensor. The mini dark box comprised a slot for inserting the holder and an adapter for connecting a smartphone used as a portable light detector (Fig. 2a-b), thus allowing to perform measurements out-of-lab without any interference from ambient light. The distance between the holder and the smartphone (about 5 cm) was long enough to permit correct focusing of the biosensor by the smartphone camera. In our experiments, we used a OnePlus 6 smartphone (OnePlus, Shenzen, China), equipped with a dual integrated camera (primary sensor: 16MP Sony Exmor RS IMX 519, BSI CMOS 1/2.6" color sensor with 1.22-µm pixels, f/1.7 aperture; secondary sensor: 20MP Sony Exmor RS IMX 376K, BSI CMOS 1/2.8" color sensor with 1.0-µm pixels, f/1.7 aperture). Images were acquired using the secondary 20MP camera.

Experiments were also performed using as light detector an ATIK 383L camera (ATIK Cameras, Norwich, England) equipped with a thermoelectrically cooled CCD sensor (8.3MP On Semiconductor (former Kodak) KAF-8300 Full Frame CCD 4/3" monochrome sensor, with 5.4-µm pixels) coupled with a Xenon 25 mm objective, f/0.95 aperture (Schneider-Kreuznach, Bad Kreuznach, Germany). In comparison with the smartphone, the higher sensitivity of the CCD camera allowed use of shorter exposure times, thus permitting a more precise characterization of the CL emission kinetics and/or detection of weak signals.

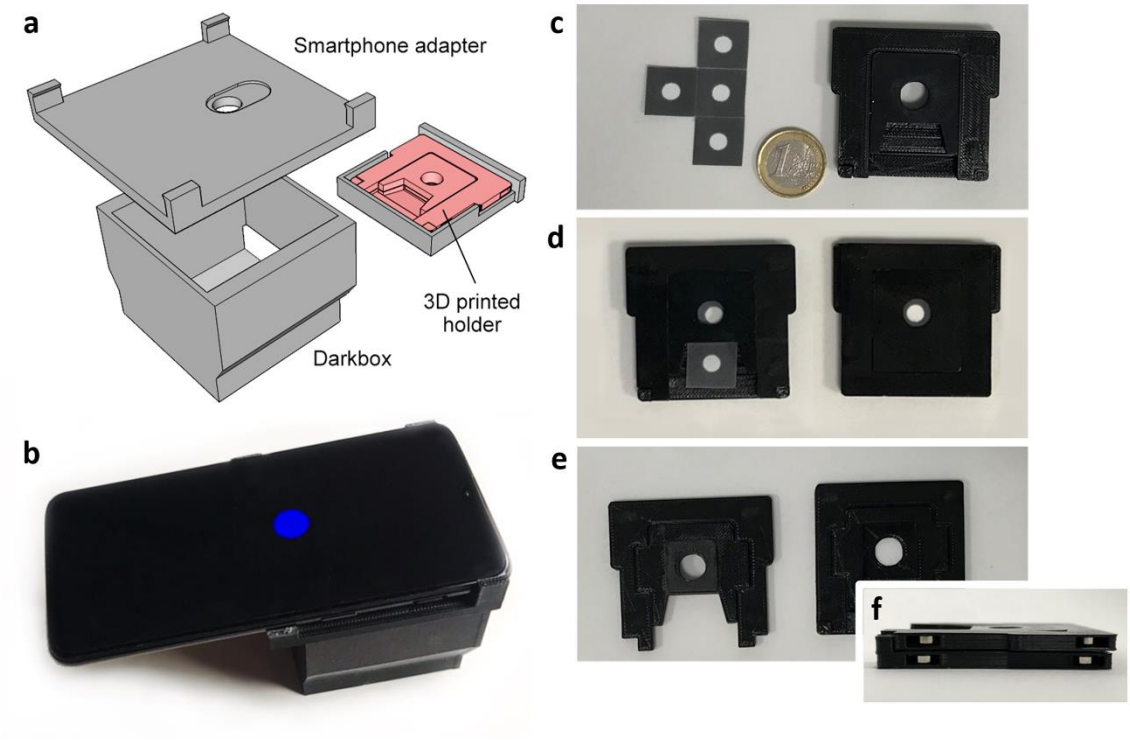

Fig. 2: a) Schematic drawing of the device. b) Device connected to the One Plus 6 smartphone. c) Unfolded paper-based biosensor and 3D printed holder. d) The two parts composing the 3D printed holder; each part contains a 5-mm hole to enable addition of luminol solution and acquisition of the CL signal with the smartphone. e) 3D printed holder (top and bottom view) housing the paper-based biosensor. f) Detail of the assembled holder showing the N52 grade neodymium magnets designed to keep the paper biosensor folded.

2.4 Assay procedure

The optimized analytical procedure for the evaluation of the activity of AChE inhibitors in a liquid sample is schematized in Fig. 1. First, a 10 µL-volume of sample is added to the well No. 1 of the biosensor (which contains the AChE enzyme) and pre-incubated for 5 minutes at room temperature so that inhibition of AChE takes place (Fig. 1a). After folding of well No. 1 on the central well (Fig. 1b) and addition of 10 µL of ACh solution (10 mM in deionized water) the AChE-catalyzed hydrolysis of ACh takes place (Fig. 1c). Then, the well No. 2 (which contains ChOx) is folded on the central well to activate the enzyme reactions leading to choline and then to hydrogen peroxide, and the partially folded biosensor is clamped by the 3D-printed biosensor holder (Fig.1d). After a second

5-min incubation, the well No. 3 containing HRP is folded on under the already stacked wells to obtain the completely folded biosensor (Fig. 1e). After clamping the biosensor in the holder again, 20 µL of a 0.025 M luminol solution in NaOH (pH 12.0) are added to trigger the final HRP-catalyzed CL reaction leading the production of the CL signal (Fig. 1f). The holder is then inserted in the mini dark box and after 10 min of incubation an image of the CL emission (30-sec exposure time, ISO 800 sensitivity) is acquired using the OnePlus 6 smartphone and saved as an RGB file.

Quantitative analysis of the CL images was performed with the open source Image J software (v. 1.52s, National Institutes of Health, Bethesda, MD, USA). A circular region of interest (ROI) was defined in the correspondence of the biosensor well and the CL signal was evaluated by integrating the CL image intensity over the ROI area (since the maximum of the CL emission is at about 460 nm, integration was performed by considering only the blue channel of the RGB image).

For all experiments, evaluation of AChE inhibition required two separate measurements, carried out either in the presence or in the absence of the inhibitor (in such case 10 µL of deionized water were used in the pre-incubation step). A blank experiment was also performed to measure the background CL signal by replacing the ACh solution with deionized water.

All measurements were performed in triplicate and repeated at least three times.

The AChE inhibition was then calculated from the CL signals as follows, where $CL_{inhibitor}$, $CL_{no\ inhibitor}$ and CL_{blank} represent the CL signals recorded in the presence and in the absence of the inhibitor and the CL background signal, respectively.

$$\text{AChE inhibition (\%)} = \frac{(CL_{no\ inhibitor} - CL_{blank}) - (CL_{inhibitor} - CL_{blank})}{(CL_{no\ inhibitor} - CL_{blank})} \times 100$$

For quantitative analysis, chlorpyrifos methyl concentrations were obtained by interpolating the AChE inhibition measured for the sample on a calibration curve generated by analyzing chlorpyrifos

methyl solutions in the concentration range 0.01 – 10.0 mM and fitting the dose/inhibition graph with a four-parameter logistic equation.

2.5 Detection of AChE in spiked food matrices and recovery study

The applicability of the foldable biosensor to the analysis of complex samples was also evaluated by detecting chlorpyrifos methyl in spiked white cabbage juice. White cabbage was chopped with a mixer and 30 g were mixed with 50 mL of deionized water and under magnetic stirring for 1 hr at room temperature (22°C) . The cabbage mush was then centrifugated at 1000 × g for 10 min and the supernatant was spiked with Reldan®22 to obtain white cabbage juice samples containing low (0.6 mM), medium (3.0 mM) and high (10.0 mM) concentrations of chlorpyrifos methyl. Spiked samples (10 µL) were then assayed with the foldable biosensor following the procedure previously described and the recovery of the assay was evaluated by comparison between the measured and spiked chlorpyrifos methyl concentrations.

2.6 Biosensor stability evaluation

Stability of the paper-based biosensor was investigated by simulating different storage and shipment conditions. A series of biosensors were produced and vacuum-packed in plastic bags by employing a simple commercial vacuum machine used to preserve food. The biosensors were stored at different temperatures, i.e., room temperature (23°C), 4°C and -20°C. At different time points (up to 30 days) sets of three biosensors stored in different conditions were tested following the procedure reported in the section “Assay procedure”. To assess biosensor stability, both the CL intensity in the absence of inhibitors and the AChE inhibition obtained in the presence of 3.0 mM chlorpyrifos methyl. The CL signals in the absence of the inhibitor and the AChE inhibitions measured in the presence of chlorpyrifos methyl were compared to those obtained at day 0, i.e., with newly produced biosensors.

3. RESULTS AND DISCUSSION

3.1 Design, fabrication and characterization of the foldable paper-based biosensor

The foldable paper-based CL biosensor allows detection of OP compounds by exploiting their capability to inhibit AChE, thus affecting the chain of coupled enzymatic reactions by decreasing the intensity of light emission:

$$Acetylcholine + H_2O \xrightarrow{AChE} Choline + Acetic\ acid \qquad (1)$$

$$Choline + O_2 \xrightarrow{ChOx} Betaine\ aldehyde + H_2O_2 \qquad (2)$$

$$H_2O_2 + Luminol \xrightarrow{HRP} Aminophthalate + N_2 + hv \qquad (3)$$

The use of cellulose chromatography paper (Whatman 1 CHR, having a pore size of 11 µm), on which wells were delimited by hydrophobic walls obtained by wax printing technique, permitted to obtain a ready-to-use biosensor containing the enzymes (AChE, ChOx, and HRP) required for the assay. Enzymes were loaded in the wells of the biosensor via adsorption by physical interactions with cellulose matrix, thus avoiding loss of catalytic activity (Hernandez and Fernandez-Lafuente, 2011; Hwang and Gu, 2013; Huang and Cheng, 2008). The values of pH of the enzyme solutions loaded in the biosensor were selected to maintain the optimal activity for the enzymes (AChE and ChOx have an optimum activity at pH 7.0 and 8.0, respectively (Kano et al., 1994). Addition of sample and reagent solutions (ACh and luminol) and sequential folding of the biosensor allowed solubilization of the enzymes loaded in the biosensor and occurrence of the enzymatic reactions (Fig. 1), from preincubation of the sample with AChE to production of H_2O_2 by exploiting the reactions catalysed by AChE and ChOx (reactions *(1)* and *(2)*). At the end, the biosensor was completely folded to obtain a single well in which the produced H_2O_2 was detected thanks to the HRP-catalyzed CL oxidation of luminol (reaction *(3)*).

3.2 Assay optimization

Several working conditions were optimized to improve the effectiveness of the foldable biosensor for measuring the AChE activity, including the diameter of the wells, the enzyme concentrations and the timing for the sequential folding to enable sequential reactions. Moreover, a luminol solution was optimized to improve CL signal detectability with the OnePlus 6 smartphone.

As concerns the biosensor design, to ensure adequate enzyme loadings two different well sizes were tested (diameter of 5 and 8 mm). A 5-mm diameter was selected for the wells since it provided a uniform CL signal. Conversely, the use of 8-mm diameter wells did not allow a uniform reaction distribution, as confirmed by the detection of CL signal only in the peripheral region of the well (Fig. S1).

Different concentrations of enzymes loaded in the biosensor (AChE from 0.5 to 1 U/well, ChOx from 0.3 to 0.6 U/well, HRP from 0.16 to 1.62 U/well) as well as of ACh (from 0.01 to 10.0 mM) were tested keeping all other factors constant (Fig. S2). This enabled to identify the conditions providing the best compromise between low reagent loading and high CL signal, thus providing a cost-effective yet sensitive tool for detection of AChE inhibitors. Higher AchE, ChOx and HRP enzyme concentrations led to a small increase in the CL emission intensity but also to higher limit of detection (LOD) of AchE inhibitors, thus the lowest enzyme concentrations were used in the assay.

To obtain a CL signal easily detectable with the smartphone-integrated CMOS camera, the effect of luminol substrate formulation on the CL emission was also studied. The commercial SuperSignal ELISA Femto Maximum Sensitivity luminol-based HRP CL substrate, which contains proprietary enhancers that improve CL emission intensity, was tested as well as home-made luminol solutions at different pH (i.e., 0.025 M luminol solutions in deionized water and NaOH solutions at pH 10.0 and pH 12.0). Indeed, the pH of the luminol solution should be a compromise between the optimal pH for HRP activity (the highest peroxidase activity is in the pH interval 6.0 - 7.0) and that for the luminol CL reaction (which is stronger at alkaline pH). To select the optimal substrate formulation and the most suitable time window for CL measurement, the CL emission in the absence of AChE inhibitors was monitored for 30 minutes after the addition of luminol substrates. As shown in Fig. 3a, thanks to

the presence of the enhancers the commercial luminol substrate provided the highest CL signal. However, despite the high signal, the fast emission kinetics drastically reduced the time window for CL signal acquisition. The strict time control required for CL measurement made such substrate not suitable for reproducible smartphone-based detection (indeed, the peak of the CL emission was not actually recorded with the OnePlus 6 smartphone). Conversely, 0.025 M luminol both in deionized water and in NaOH solution pH 10.0 showed weak CL signals, which were hardly detectable with the OnePlus 6 CMOS camera. The luminol solution in NaOH at pH 12.0 proved the most suitable for smartphone-based measurement: even though the CL signal intensity was lower than obtained with the SuperSignal ELISA Femto substrate, the CL emission was still easily detectable by the smartphone and it showed a glow-type kinetics. Indeed, the CL signal remained almost constant between 10 and 20 minutes after the addition of the substrate, thus facilitating the measurement. In accordance to the CL signal kinetics, all CL measurements were performed 10 minutes after the addition of the luminol substrate.

It should be noted that the selected pH value is higher than the optimal pH value reported in the literature for the luminol/H_2O_2/HRP system (between pH 9.5 and pH 10.0 according to Khan et al., 2014), but the discrepancy could be due to the partial neutralization of NaOH by the buffers loaded into the biosensor with the AChE and ChOx enzyme solutions.

Once selected the optimal experimental conditions for performing H_2O_2 detection with the smartphone camera, we optimized the incubation time of ACh with AChE and ChOx. As shown in Fig. 3b, CL signals were proportional to the reaction time up to 15 minutes, but their intensities remained in the same order of magnitude. As the best compromise in terms of detectability of the CL signal with the smartphone and time-saving analysis, a reaction time of 5 min was selected.

As a performance test of the foldable paper biosensor, we obtained a dose-response curve for ACh. To this end, 10 µL-volumes of ACh solutions (concentration range 0.01 - 10.0 mM) were analyzed in triplicate with the foldable biosensor and the CL measurements were performed with the ATIK 383L CCD camera, using both luminol solutions at pH 10.0 and pH 12.0. Fig. 3c illustrates CL signals

obtained with different ACh dilutions, showing as expected stronger CL signals with the luminol solution in NaOH pH 12.0, thus confirming the suitability of this luminol solution for smartphone-based detection. By using the latter luminol solution, a LOD for ACh, calculated as 3 times the standard deviation of the blank (deionized H_2O), of 160 µM was obtained.

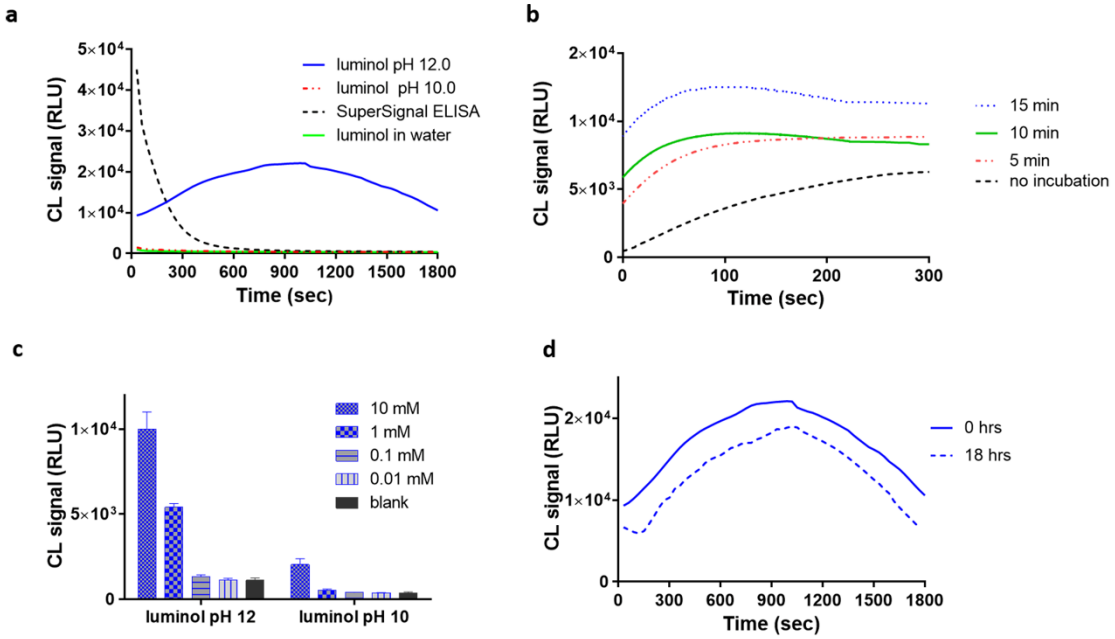

Fig.3: a) CL emission kinetics of the paper-based biosensor obtained with four different substrates (the commercial SuperSignal ELISA Femto substrate and 0.025 M luminol in water and in NaOH solutions at pH 10.0 and pH 12.0). CL measurements were performed with CCD ATIK 383L- camera integrating CL signals for 30 sec at room temperature. b) Optimization of the incubation time (from 0 to 15 min) of ACh (10mM) with the AChE and ChOx previously adsorbed on the paper biosensor. CL emission kinetics were obtained with CCD ATIK 383L- camera integrating CL signals (30 sec at room temperature) after the addition of luminol solution at pH 12.0; c) Dose-response curves for Ach obtained with the paper-based biosensor (concentration range 0.01-10.0 mM). CL measurements were performed with ATIK 383L CCD (integration time of 30-sec at room temperature) after 10 min of the addition of home-made luminol pH 12.0 and normal luminol pH 10.0; d) Comparison of CL emission kinetics obtained with the paper-based biosensor without storage (0 hrs) and after 18 hrs storage at room temperature using a CCD ATIK 383L-camera (CL signal integration of 30 sec at room temperature).

3.3 Evaluation of AChE inhibition

To prove the suitability of the biosensor to evaluate AChE inhibition, a simulated inhibition experiment was performed by measuring the CL signal obtained from biosensors in which decreasing amounts of AChE (starting from 0.5 U/well, i.e., the concentration used in the biosensor) were loaded in the biosensor. The experiments were performed in the optimized experimental conditions without AChE inhibitor (replaced by deionized H_2O) and the CL signal was correlated to the amount of AChE in the biosensor. As shown in Fig. 4a, the intensity of the CL signal showed a linear correlation with the amount of AChE, thus suggesting that comparison of the CL signals obtained in the presence and in the absence of an inhibitor allowed to estimate the AChE inhibition (indeed, the relative decrease of the CL signal represented the actual inhibition of AChE). Considering the reproducibility of the CL measurements, it can be assumed that AChE inhibitions as low as 15% could be reliably detected with the developed foldable biosensor.

3.4 Detection of AChE inhibitors

The suitability of the smartphone-based foldable biosensor to detect AChE irreversible inhibitors was investigated using chlorpyrifos methyl as a model OP pesticide able to irreversibly inhibit AChE. Chlorpyrifos methyl is an OP pesticide commonly used in agriculture, for which exposure may occur either directly or via the food chain. Several commercial pesticides contain chlorpyrifos methyl, including Reldan®22, a broad-spectrum insecticide for control of insects and mites containing 225 g/L of chlorpyrifos methyl.

To obtain a calibration curve suitable for quantitative analysis of chlorpyrifos methyl, spiked Reldan®22 solutions in water corresponding to chlorpyrifos methyl concentrations in the range 0.01 – 10.0 mM were analyzed using the procedure described in section “Analytical procedure”. A stated before, because we correlated the concentration of OP compounds with the decrease of the biosensor response upon enzyme inhibition, each experiment was conducted by comparing the CL signals obtained in the presence and in the absence of the inhibitor.

Before generating the dose-response curve, the incubation time of the biosensor with the sample was optimized by analyzing an intermediate concentration sample (3.0 mM chlorpyrifos methyl) after different incubation times with AChE and comparing the CL signals with that obtained from the control without pesticide (10 µL of deionized water). As shown in Fig. 4b, the irreversible inhibition by the pesticide is almost immediate and the decrease in the CL signal reached a constant value upon only 5 min of incubation. This incubation time was thus used in the subsequent experiments.

Fig. 4c showed representative CL images obtained for the various chlorpyrifos methyl concentrations and the corresponding dose-response curve generated as reported in Section 2.4. According to the dose-response curve, the LOD for chlorpyrifos methyl was 45.0 µM. When compared to other biosensors for OP detection relying on amperometric and potentiometric detection (Pundir and Malik, 2019), our CL paper-based biosensor provided a higher LOD. In fact, reported limits of detection ranged from µM to sub-nM for different OPs; however, it must be pointed out that the smartphone-based biosensor is intended to be a low-cost device to be used without any specialized laboratory instrumentation. In the last five years CL has been used as detection technique for a limited number of smartphone-based biosensors, mainly for nucleic acid and immunosensors (Ghosh et al., 2020; Kalligosfyri et al., 2019). To the best of our knowledge this is the first CL enzyme paper-based smartphone-integrated biosensor. In comparison with a previously reported CL enzyme smartphone biosensor for lactate that provided LOD at the mM level (Roda et al, 2014b), we were able to significantly improve detectability, thus confirming that this approach is suitable for smartphone-based sensing, although its full potential has yet to be reached.

As additional feature, this paper-based “green biosensor” can be easily produced in any laboratory (only an office wax printer is required) in a sustainable way and disposed after use without safety concerns. Most importantly, the foldable paper biosensor is highly versatile and, by proper selection of the loaded enzymes, it could be easily repurposed to obtain low-cost disposable cartridges for detecting analytes in a rapid and simple way.

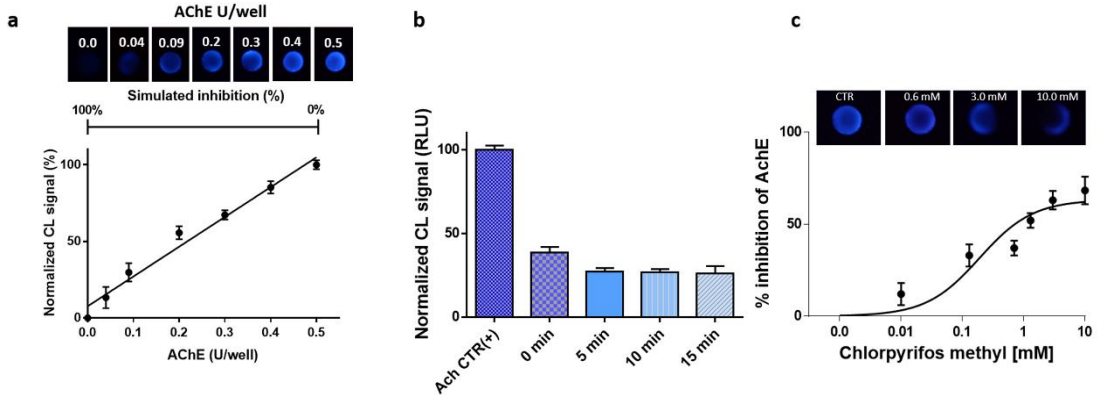

Fig. 4: a)Simulated inhibition curve performed by measuring the CL signal obtained with paper-based biosensors in which decreasing amounts of AChE (from 0.5 U to 0.04 U) were previously adsorbed in well No. 1. In optimized experimental conditions CL signals were obtained with OnePlus6 smartphone (ISO 800, 30 sec) after 10 minutes of substrate reaction and analyzed with ImageJ Software; b) Optimization of the pre-incubation time with the OP with the paper-based biosensor. Several incubation times (0, 5, 10, and 15 min) of chlorpyrifos-methyl (3.0 mM) were evaluated with the origamiPAD biosensor and CL measurement were performed with CCD ATIK 383L- camera integrating CL signals for 30 sec at room temperature after 10 minutes of luminol solution at pH 12.0. The obtained CL signals were compared with the control, without pesticide (10 µL of water solution); c) Chlorpyrifos-methyl inhibition curve obtained with the foldable biosensor testing a concentration range of Reldan® 22 suggested by the manufacturer (concentration range of chlorpyrifos-methyl from 0.01 to 10 mM in deionized water). CL images corresponding to the Chlorpyrifos-methyl inhibition curve were obtained acquiring CL signals with Oneplus 6 camera after 10 minutes of substrate reaction (ISO 800, 30 sec) and analyzed with ImageJ Software.

3.5 Recovery in spiked samples

To investigate potential matrix effects and evaluate the performance of the developed foldable biosensor for detection of pesticides in real samples, a recovery study was carried out on a vegetable sample (i.e., white cabbage juice). White cabbage juice samples were spiked with Reldan® 22 at three different chlorpyrifos-methyl concentrations (0.6, 3.0 and 10.0 mM) and analyzed with the foldable biosensor. The recovery values for chlorpyrifos methyl (Table S1) were in the range 92% - 99%, thus suggesting a low matrix effect and further confirming the suitability of the proposed biosensor for real sample analysis. Conversely, no OPs were detected in blank white cabbage juice.

3.6 Biosensor precision and stability

Different figures of merit of the biosensor including repeatability, reproducibility and stability and were studied. As concerns the repeatability, a relative standard deviation (RSD, n = 5) of 9.8 % was obtained for biosensors produced in the same day and used for detecting an intermediate concentration (3.0 mM) of chlorpyrifos-methyl. Conversely, a reproducibility (RSD, n = 5) of 13.2% was obtained by analysing the same sample in consecutive days using biosensors produced in the same day and maintained until use in the optimal storage conditions (see below).

As concerns biosensor stability, Fig. 5b shows the CL signals measured for biosensors vacuum-packed in plastic bags and stored at different temperatures (22°C, 4°C and -20°C) and for different periods of time (up to 30 days). The measurements were performed in the optimized experimental conditions without any AChE inhibitor and, for reference, the CL signals have been normalized to the value obtained immediately after the production of the biosensors. Storage of the biosensors at room temperature (22°C) or at 4°C resulted in a decrease of the CL signal, which is reasonably due to a loss of enzyme activity. After 48 h at room temperature the loss of the CL signal was 35 ± 5 %, while a smaller, but still significant, reduction (20 ± 6%) was observed during storage at +4°C. After one week the decreases of the CL signals were 61 ± 3% and 19 ± 4% at room temperature and 4°C, respectively. Conversely, storage at –20°C proved suitable for long-term storage of the biosensors since after 30 days we observed a decrease of the CL signal of only 2 ± 3%. Additionally, the overall kinetics of the CL emission remained unchanged upon storage at -20°C for up to 30 days.

Short-term stability at room temperature was also investigated to confirm that the biosensor remained usable for a reasonable time after unpacking. As shown in Fig. 5a the catalytic activity of the enzymes, as well as the overall kinetics of the CL emission, were maintained stable after up to 18 h of storage of the unpacked biosensor at 22°C, with a decrease of the CL signal of 20 ± 3 %.

These results support the fact, if adequately refrigerate, that the biosensor has an adequate shelf-life to allow storage and shipping.

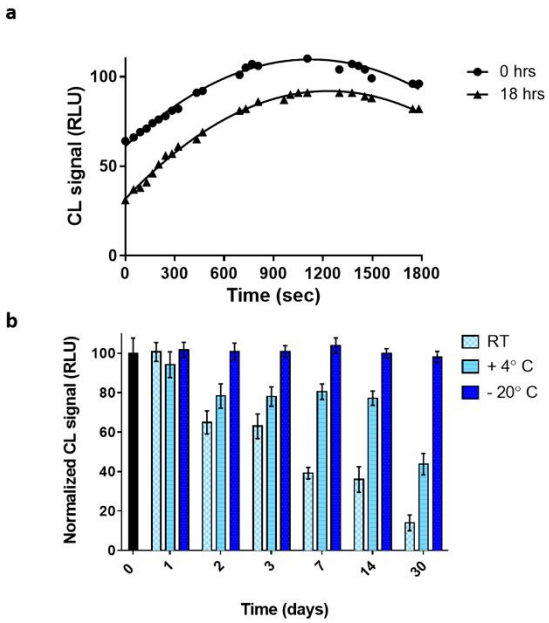

Fig. 5: a) Comparison of CL emission kinetics of the paper-based biosensor obtained with the biosensor without storage (0 hrs) and after 18 hrs storage at room temperature. CL measurements were performed using the maximum performance settings of OnePlus6 smartphone (30 s, ISO 800) and CL images were elaborated by ImageJ Software; b) Stability of the paper-based biosensor stored at room temperature (23°C), +4°C and -20°C. Each indicated day (from 0 to 30 days), triplicate paper-based biosensors were tested following the procedure reported in the section "Assay procedure". CL measurements were obtained with OnePlus 6 (30 s at ISO 800) and analyzed with ImageJ software. CL signals are normalized with respect to day 0.

Conclusions

We presented a foldable CL paper biosensor that capitalizes on well-established assays based on enzyme inhibition, sensitive CL detection relying on luminol/H_2O_2/HRP system, foldable paper biosensors and the possibility to use the smartphone integrated CMOS as light detector. We integrated for the first time these concepts to provide a CL biosensor that enables a very rapid and

straightforward analysis of compounds inhibiting AChE, by exploiting coupled enzymatic reactions involving AChE, ChOx and HRP and an improved luminol solution as the CL substrate.

The biosensor here described allows the measurement of the AChE inhibitory activity in very short times (less than 30 min) using small volumes of samples and, thanks to high intensity of the CL signal, enables smartphone-based detection. Thanks to the 3D printing technology, biosensor's housing interfacing with smartphone is straightforward and different smartphone adaptors can be easily designed and produced according to various smartphone models.

Biosensor validation was performed using chlorpyrifos methyl and spiked cabbage juice samples, showing its potential applicability to rapidly detect the presence of OP pesticides along the food chain. Moreover, the developed biosensor could be applied to replace currently employed colorimetric papers used to rapidly detect nerve agents and OP insecticides.

Acknowledgements

This research was sponsored in part by the PRIN 2015 project Prot. 2015FFY97L and the NATO Science for Peace and Security Programme under Grant No. 985042.

References

Ahmed, N.Y., Knowles, R., Dehorter, N., 2019 Front Mol Neurosci 12:204.

Andreani, A., Burnelli, S., Granaiola, M., Guardigli, M., Leoni, A., Locatelli, A., Morigi R., Rambaldi M., Rizzoli M., Varoli L., Roda, A., 2008. Euro. J. Med. Chem. 43, 657-661.

Andreani, A., Granaiola, M., Guardigli, M., Leoni, A., Locatelli, A., Morigi, R., Rambaldi M., Roda, A., 2005. Euro. J. Med. Chem. 40, 1331-1334.

Arduini, F., Amine, A., Moscone, D., Palleschi, G., 2010. Micro. Acta 170, 193-214.

Arduini, F., Cinti, S., Caratelli, V., Amendola, L., Palleschi, G., Moscone, D., 2019. Biosens Bioelectron., 126, 346-354. Calabretta, M. M., Álvarez-Diduk, R., Michelini, E., Roda, A., and Merkoçi, A., 2020. Biosens Bioelectron., 150, 111902.

Capoferri, D., Della Pelle, F., Del Carlo, M., Compagnone, D., 2018. Foods 7, 148.

Cavusoglu, K., Celik, H., Senturk, M., Ekinci, D., 2016. Acta Physio. 218.

Cevenini, L., Calabretta, M. M., Lopreside, A., Tarantino, G., Tassoni, A., Ferri, M., Roda, A., Michelini, E., 2016. Anal. Bioanal. Chem. 408, 8859-8868.

Chang, J., Li, H., Hou, T., Li, F., 2016. Biosens Bioelectron. 86, 971-977.

Chen, Z., Tan, Y., Xu, K., Zhang, L., Qiu B., Guo, L, Lin, Z., Chen, G. 2016. Biosens Bioelectron. 75:8-14.

Cinti, S., 2019. Anal. Bioanal. Chem. 411, 4303-4311.

Clegg, D. L., 1950. Anal. Chem. 22, 48-59.

Colovic, M. B., Krstic, D. Z., Lazarevic-Pasti, T. D., Bondzic, A. M., Vasic, V. M., 2013. Curr. Neuropharmacol. 11, 315-335.

Colozza, N., Kehe, K., Dionisi, G., Popp, T., Tsoutsoulopoulos, A., Steinritz, D., Moscone D., Arduini, F., 2019. Biosens. Bioelectron. 129, 15-23.

Comer, J. P., 1956. Anal. Chem. 28, 1748-1750.

Cui, H. F., Zhang, T. T., Lv, Q. Y., Song, X., Zhai, X. J., & Wang, G. G., 2019. Biosens. Bioelectron. 141, 111452.

Dehorter, N., 2019. Front. Mol. Neuro. 12, 204.

Del Carlo, M., Mascini, M., Pepe, A., Compagnone, D., Mascini, M., 2002. J. Agri. Food Chem. 50, 7206-7210.

Deng, Y., Zhang, Y., Lu, Y., Zhao, Y., & Ren, H., 2016. Sc. Tot. Env. 544, 507-514.

Devi, D. L., Burkhard. R., J. Justin Gooding 2 and Edith Chow 1, Sensors 2012, 12(9), 11505-11526

Fenoy, G. E., Marmisollé, W. A., Azzaroni, O., Knoll, W., 2020. Biosens. Bioelectron. 148, 111796.

Garlito, B., Ibáñez, M., Portolés, T., Serrano, R., Amlund, H., Lundebye, A. K., Sanden, M., Berntssen, M. H. G., Hernández, F., 2019. Anal. Bioanal. Chem. 411, 7281-7291.

Ge, L., Wang, S., Song, X., Ge, S., Yu, J., 2012. Lab Chip 12, 3150-3158.

Ghosh, S., Aggarwal, K., Vinitha, T.U., Nguyen, T., Han, J., Ahn, C.H. 2020, Microsyst & Nanoeng, 6-5

Guardigli, M., Pasini, P., Mirasoli, M., Leoni, A., Andreani, A., Roda, A., 2005. Anal. Chim. Acta 535, 139-144.

Guilbault, G. G., Kramer, D. N., Cannon Jr, P. L., 1962. Anal. Chem. 34, 1437-1439.

He, Y., Du, J., Luo, J., Chen, S., Yuan, R., 2020. Biosens. Bioelectron. 150, 111898.

Hernandez, K., Fernandez-Lafuente, R., 2011. Enzym. Microb. Technol. 48, 107–122.

https://ec.europa.eu/food/plant/pesticides/approval_active_substances/chlorpyrifos_chlorpyrifos-methyl_en

Hu, J., Wang, S., Wang, L., Li, F., Pingguan-Murphy, B., Lu, T.J., Xu, F., 2014. Biosens Bioelectron. 54, 585-97.

Huang, L., Cheng, Z. M., 2008. Chem. Eng. J. 144, 103-109.

Huang, S., Yao, J., Chu, X., Liu, Y., Xiao, Q., Zhang, Y., 2019. J. Agri. Food Chem. 67, 11244-11255.

Huang, X., Xu, D., Chen, J., Liu, J., Li, Y., Song, J., Ma, X., Guo, J., 2018. Analyst 143, 5339-5351.

Hwang, E. T., Gu, M. B., 2013. Eng. Life Sciences 13, 49-61.

Jin, L., Hao, Z., Zheng, Q., Chen, H., Zhu, L., Wang, C., Liu, X., Lu, C., 2020. Anal. Chim. Acta 1100, 215-224.

Kalligosfyri, P.M., Sevastou, A., Kyriakou, I.K., Tragoulias, S.S., Kalogianni, D.P., Christopoulos T.K., 2019 Anal Chim Acta. 1088, 123-130.

Kano, K., Morikage, K., Uno, B., Esaka, Y., & Goto, M., 1994. Anal. Chim. Acta 299, 69-74.

Khan, P., Idrees, D., Moxley, M. A., Corbett, J. A., Ahmad, F., von Figura, G., Sly, W. S., Waheed, A., Hassan, M. I., 2014. Appl. Biochem. Biotechnol. 173, 333-355.

Li, F., Liu, J., Guo, L., Wang, J., Zhang, K., He, J., Cui, H., 2019. Biosens Bioelectron. 141:111472.

Liana, D. D., Raguse, B., Gooding, J. J., Chow, E., 2012. Sensors 12, 11505-11526.

Liang, B., Han, L., 2020. Biosens. Bioelectron. 148, 111825.

Liu, W., Cassano, C. L., Xu, X., Fan, Z. H., 2013. Anal. Chem. 85, 10270-10276.

Liu, X., Li, X., Gao, X., Ge, L., Sun, X., Li, F., 2019. ACS Appl Mater Interfaces. 11, 15381-15388.

López-Marzo, A.M., Merkoçi, A., 2016 Lab Chip. 16:3150-76

Martinez, A. W., Phillips, S. T., Whitesides, G. M., 2008. PNAS 105, 19606-19611.

Martinez, A. W., Phillips, S. T., Whitesides, G. M., Carrilho, E., 2010. Anal. Chem. 82, 1, 3-10.

Meredith, N. A., Quinn, C., Cate, D. M., Reilly, T. H., Volckens, J., & Henry, C. S., 2016. Analyst 141, 1874-1887.

Patel, S., Sangeeta, S., 2019. ESPR 26, 91-100.

Pundir, C. S., Malik, A., 2019. Biosens. Bioelectron. 111348.

Qureshi, S. Z., Ahmad, S. T., Haque, S., 1990. Talanta 37, 763-765.

Roda, A., Calabretta, M. M., Calabria, D., Caliceti, C., Cevenini, L., Lopreside, A., and Zangheri, M., 2017. Smartphone-Based Biosensors, in: Comprehensive Analytical Chemistry, Past, Present and Future Challenges of Biosensors and Bioanalytical Tools in Analytical Chemistry: A Tribute to Professor Marco Mascini, pp. 237-286.

Roda, A., Guardigli, M., Calabria, D., Calabretta, M.M., Cevenini, L., Michelini, E., 2014b. Analyst. 139, 6494-501

Roda, A., Michelini, E., Cevenini, L., Calabria, D., Calabretta, M. M., Simoni, P., 2014a. Anal. Chem. 86, 7299-7304.

Roda, A., Michelini, E., Zangheri, M., Di Fusco, M., Calabria, D., Simoni, P., 2016. TrAC 79, 317-325.

Roda, A., Rauch,P., Ferri, E., Girotti, S., Ghini, S., Carrea, G., Bovara, R., 1994. Anal. Chim. Acta, 294, 35-42

Rorem, E. S., Lewis, J. C. ,1962. Anal. Biochem. 3, 230-235.

Samsidar, A., Siddiquee, S., Shaarani, S. M., 2018. Trends Food Sci. Technol. 71, 188-201.

Uniyal, S., Sharma, R. K., 2018. Biosens. Bioelectron. 116, 37-50.

Yao, T., Liu, A., Liu, Y., Wei, M., Wei, W., Liu, S., 2019. Biosens. Bioelectron. 145, 111705.

Yeh. H.W., A,i H.W., 2019. Annu Rev Anal Chem (Palo Alto Calif). 12, 129-150.

Zangheri, M., Cevenini, L., Anfossi, L., Baggiani, C., Simoni, P., Di Nardo, F., Roda, A., 2015. Biosens. Bioelectron. 64, 63-68.

Zilbeyaz, K., Stellenboom, N., Guney, M., Oztekin, A., Senturk, M., 2018. J. Biochem. Mol. Toxicol. 32, e22210.